



## ORIGINAL ARTICLE

# CuO NPs@Starch as a novel chemotherapeutic drug for the treatment of several types of gastrointestinal system cancers including gastric, pancreatic, and colon cancers



Jianpeng Chen <sup>a</sup>, Bikash Karmakar <sup>b,\*</sup>, Mohamed A. Salem <sup>c,d</sup>,  
Abdullah Y. Alzahrani <sup>c</sup>, Mutasem Z. Bani-Fwaz <sup>e</sup>, Mohamed M. Abdel-Daim <sup>f,g</sup>,  
Attalla F. El-kott <sup>h,i</sup>

<sup>a</sup> Department of Oncology, Shandong Provincial Hospital affiliated to Shandong First Medical University, Jinan 250021, China

<sup>b</sup> Department of Chemistry, Gobardanga Hindu College, 24-Parganas (North), India

<sup>c</sup> Department of Chemistry, Faculty of Science & Art, King Khalid University, Mohail, Assir, Saudi Arabia

<sup>d</sup> Department of Chemistry, Faculty of Science, Al-Azhar University, 11284 Nasr City, Cairo, Egypt

<sup>e</sup> Department of Chemistry, Faculty of Science, King Khalid University, P. O. Box 9004, Abha 61413, Saudi Arabia

<sup>f</sup> Pharmaceutical Sciences Department, Pharmacy Program, Batterjee Medical College, P.O. Box 6231, Jeddah 21442, Saudi Arabia

<sup>g</sup> Pharmacology Department, Faculty of Veterinary Medicine, Suez Canal University, Ismailia 41522, Egypt

<sup>h</sup> Biology Department, College of Science, King Khalid University, Abha 61421, Saudi Arabia

<sup>i</sup> Zoology Department, College of Science, Damanhour University, Damanhour 22511, Egypt

Received 13 June 2021; accepted 29 December 2021

Available online 4 January 2022

## KEYWORDS

CuO nanoparticles;  
Starch;  
Gastric cancer;  
Pancreatic cancer;  
Colon cancer

**Abstract** Copper oxide nanoparticles were successfully synthesized through a simple and 'green' route using starch as a capping and stabilizing agent under ultrasonic irradiation in alkaline medium. Unique reaction condition was prepared by ultrasonic irradiation, releasing the stored energy in the collapsed bubbles and heats the bubble contents that leads to Cu(II) reduction in the presence of starch. The obtained nanoparticle (CuO NPs@Starch) was characterized by advanced physical and chemical techniques like Transmission Electron Microscope (TEM), Fourier-transform infrared spectroscopy (FTIR), Uv-Vis spectroscopy, scanning electron microscopy (SEM), X-ray Diffraction (XRD) and energy-dispersive X-ray analysis (EDX). The properties of CuO

\* Corresponding author.

E-mail address: [bikashkarm@gmail.com](mailto:bikashkarm@gmail.com) (B. Karmakar).

Peer review under responsibility of King Saud University.



Production and hosting by Elsevier

NPs@Starch against gastric cancer (AGS and KATO III), pancreatic cancer (AsPC-1 and MIA PaCa-2), and colon cancer (HCT 116 and HCT-8) were evaluated. The viability of malignant cancer cell lines reduced dose-dependently in the presence of CuO NPs@Starch. After clinical study, CuO NPs@Starch can be utilized as an efficient drug in the treatment of gastric, pancreatic, and colon cancers in humans.

© 2021 Published by Elsevier B.V. on behalf of King Saud University. This is an open access article under the CC BY-NC-ND license (<http://creativecommons.org/licenses/by-nc-nd/4.0/>).

## 1. Introduction

Cancer is a deadly disease with high mortality that leads to many psychological and economic conflicts. Lifestyle is one of the most important and effective factors in the incidence of cancer. Environmental factors such as environmental pollutants, carcinogens and mutagens, bacterial and viral infections as well as genetic susceptibility are the most important factors in the incidence of cancer (Borm et al., 2006; De Jong and Borm, 2008; Mao, 2016; You et al., 2012). Depending on the type of cancer, the extent of the disease and the patient's condition, a combination of different methods such as surgery, radiotherapy and chemotherapy are used to fight and control cancer. Despite the possibility of side effects in advanced cancers, most of these common methods do not produce positive results and the need for research and finding new ways to fight cancer is urgently needed (Borm et al., 2006; De Jong and Borm, 2008; Mao, 2016; You et al., 2012; Trojer et al., 2021; Liu et al., 2014). Nanotechnology is the efficient production of materials, devices and systems by controlling matter at the nanometer scale and exploiting new properties and phenomena that have been developed at this scale. Nanoparticles are atomic or molecular assemblies with minimum dimensions between 1 and 100 nm with different physicochemical properties compared to the mass of their material. Nanotechnology has been instrumental in developing a new cancer treatment strategy (Trojer et al., 2021; Liu et al., 2014; Tong et al., 2004).

Metal nanoparticles are known to be strong antifungal, antimicrobial and disinfectant substances. There are different applications and methods for chemical, physical and biological synthesis of nanoparticles (Baran et al., 2017; Wang et al., 2014; Elkhenany et al., 2020; Veisi et al., 2021a; Budarin et al., 2008). Among them are biological methods of nanoparticle synthesis, which means using natural resources to synthesize nanoparticles, due to the high costs of the chemical synthesis processes and dependence on environmentally harmful chemical compounds, it is important to study the biological synthesis of nanoparticles with low energy consumption and cost compared to chemical methods and without the need for organic solvents (Wang et al., 2014; Elkhenany et al., 2020; Veisi et al., 2021a; Budarin et al., 2008; Shaabani et al., 2008). The biosynthesis of metallic nanoparticles has been studied using various biological sources. But one of the problems with these synthesized nanoparticles is their instability, which lasts about three months on average (Baran et al., 2017; Wang et al., 2014; Elkhenany et al., 2020; Veisi et al., 2021a).

Between the biomolecular structures, natural biopolymers can be used to manufacture biomolecules-functionalized nanocomposites because these materials are renewable, available, chemically stable, and, most importantly, eco-friendly.

Starch is one of the natural biopolymers and belongs to the polysaccharides produced by green plants (Tong et al., 2004; Baran et al., 2017; Wang et al., 2014). Due to starch features such as biocompatibility, biodegradability, high charge density, and small size compared to other coating polymers, it is introduced as a proper support for synthesis and stabilizing metal nanoparticles. Furthermore, starch is an economical, non-toxic, and available natural polymer that can readily undergo chemical modification and stabilize nanoparticles due to its large number of free hydroxyl groups (Elkhenany et al., 2020; Veisi et al., 2021a; Budarin et al., 2008; Shaabani et al., 2008).

In this work, we have proposed the 'green' approach for synthesis of stable starch capped copper nanoparticles (CuO NPs@Starch) with desirable biological properties (Scheme 1). We investigated the nanocomposite in the cytotoxicity and anti-cancer studies against common gastric cancer (AGS and KATO III), pancreatic cancer (AsPC-1 and MIA PaCa-2), and colon cancer (HCT 116 and HCT-8).

## 2. Experimental

### 2.1. Materials and methods

The chemicals required for catalyst synthesis and catalyst applications were purchased from Sigma Aldrich.

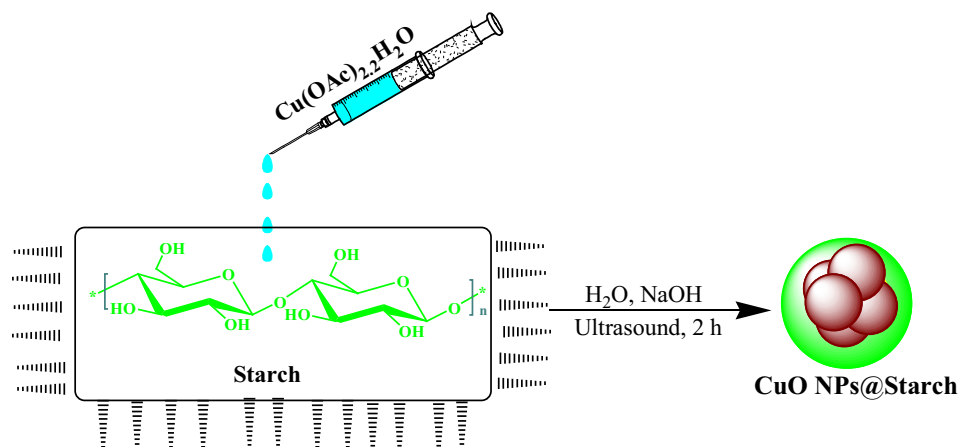
### 2.2. Synthesis of CuO NPs@Starch

To initiate the reaction 50 mL of a freshly prepared aqueous solution of  $\text{Cu}(\text{OAc})_2 \cdot 2\text{H}_2\text{O}$  (10 mM) was added to 100 mL of an aqueous starch solution under ultrasonic conditions and left for 10 min at 60 °C. Then pH of the solution was adjusted to 10.0 (NaOH, 3 wt%) and the reaction mixture was kept with sonication at 60 °C for 2 h. The progress of the reaction could be monitored by change in color blue ( $\text{Cu}^{2+}$  ion) to dark brown (CuO NP). The prepared CuO NPs@Starch was collected by centrifugation and washed several times with DI-water.

### 2.3. Anti-cancer properties of CuO NPs@Starch

The cytotoxic effects of synthesized CuO NPs@Starch on common cancer cell lines i.e. gastric cancer (AGS and KATO III), pancreatic cancer (AsPC-1 and MIA PaCa-2), and colon cancer (HCT 116 and HCT-8) were assessed using MTT colorimetric method.

For this purpose, each cell line was placed separately in T25 flasks with a complete culture medium (including DMEM (Dulbecco's Modified Eagle Medium, 10% complementary bovine fetal serum, and 1% penicillin-streptomycin solution)



**Scheme 1** Synthesis of CuO NPs@Starch under ultrasound conditions.

and at 37 °C in the incubator, cell culture was incubated with 5% CO<sub>2</sub>. After obtaining 80% cell density, the sample was exposed to 1% trypsin-EDTA solution and after 3 min of incubation at 37 °C in a cell culture incubator with 5% CO<sub>2</sub> and observation of cells removed from the bottom of the plate, the sample was centrifuged at 5000 rpm for 5 min and then the cell precipitate was decryped by adding trypsin culture medium. Then, the cell suspensions after adding trypan blue dye were counted by neobar slide and cytotoxicity test was performed by MTT method (Veisi et al., 2021b).

Initially, 10,000 cells were implanted in cell culture plates and then the cells were treated at concentrations of 1–1000 µg/mL of CuO NPs@Starch. After 24 h, 20 µL of MTT dye was added to the wells and incubated for 5 h at 37° C with 5% CO<sub>2</sub>. DMSO was then added to the wells to dissolve the formazan crystals and the absorption rate of the wells at 570 nm was read by ELISA reader (ELISA Teknika Oraganon reader, Netherlands) and the cell viability rate was computed by the below formula (Lu et al., 2021):

$$\text{Cell viability (\%)} = \frac{\text{Sample A.}}{\text{Control A.}} \times 100$$

Then, based on the absorption rate of each well and its comparison with the control, the inhibitory concentration of 50% (IC<sub>50</sub>) was obtained (Lu et al., 2021).

#### 2.4. Measurement of DPPH radical inhibitory potency

The use of DPPH radical to study the antioxidant properties of nanoparticles containing medicinal natural antioxidants in general has become one of the most widely used methods for measuring antioxidant power. The reason for this is the simplicity and high sensitivity of this method. This test is based on the theory that the hydrogen donor is an antioxidant. This radical shows its highest absorption at the wavelength of 517–515 nm. Radical DPPH is converted from an antioxidant to a stable (non-radical) DPPH due to hydrogen uptake. As a result of this conversion, its color gradually changes from dark purple to light yellow, and as a result, the absorption decreases at 517–515 nm. Therefore, the measurement of antioxidant power can be easily measured and estimated by the spectrometer by calculating the amount of absorption reduction at a wavelength of 517–515 nm. An index called IC<sub>50</sub> can also be used to report the antioxidant potency obtained according to

this method. This index indicates the concentration of antioxidants required to reduce the concentration of primary DPPH radicals by 50%. In this study, the anti-radical activity of the studied CuO NPs@Starch was performed using stable DPPH radicals according to Lu et al. and at a wavelength of 517 nm. The amount of radical removal activity was determined using the following formula (Lu et al., 2021):

$$\text{Inhibition (\%)} = \frac{\text{Sample A.}}{\text{Control A.}} \times 100$$

In this regard, the blank adsorption indicates the adsorption of the control solution, which contains 0.5 mL of DMPH solution and 100 µL of 95% ethanol instead of CuO NPs@Starch solution and adsorption of the reaction indicates the adsorption of the solution content of the CuO NPs@Starch sample (Lu et al., 2021).

### 3. Results and discussion

#### 3.1. Structural characterization of CuO NPs@Starch nanocomposite

The as synthesized CuO NPs@Starch nanocomposite was characterized using UV–Vis and FT-IR spectroscopy,

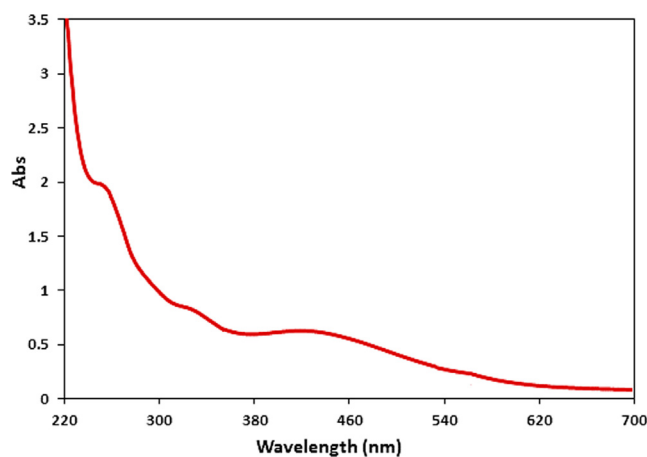


**Fig. 1** UV–visible absorption spectra of CuO NPs@Starch nanocomposite.

FESEM, TEM, XRD and EDX study. The successful biogenic synthesis of CuO NPs was primarily assured by visual color change from blue to dark brown. The formation of CuO NPs was further justified from UV–Vis spectroscopy. Fig. 1 displays the typical plasmon resonance band of CuO NP, being observed at  $\sim 400$  nm ( $\lambda_{\text{max}}$ ) (Veisi et al., 2021b).

Fig. 2 displays the FT-IR spectra of starch and CuO NPs@Starch nanocomposite. In the FT-IR spectra of starch (Fig. 2a) the broad peak appeared at  $3444$   $\text{cm}^{-1}$  corresponds to the overlapped stretching vibrations of OH groups. The alcoholic C–O stretching and O–H bending peaks are observed at  $1077$   $\text{cm}^{-1}$  and  $1658$   $\text{cm}^{-1}$  respectively. Fig. 2b represents the corresponding peaks of CuO NPs@Starch. It resembles very much to Fig. 2a, which justifies the unmodified core structure even after Au deposition over starch. However, all the characteristic peaks of CuO NPs@Starch are somewhat shifted to higher or lower wavelength regions compared to starch peaks. This is attributed to the strong complexation of CuO NPs with the starch and OH functions. These groups in turn act as stabilizing caps for the CuO NPs.

The particle size, shape, texture and surface morphology of the CuO NPs@Starch nanocomposite was ascertained by FE-SEM study, as shown in Fig. 3. It displays the quasi-spherical shaped nanoparticles of mean diameter 20–30 nm. All the particles are of uniform shape and texture. For further structural inheritance of the nanocomposite, TEM analysis was carried out (Fig. 4). The TEM measurements revealed the presence of spherically shaped nanoparticles in the matrix (Fig. 4). The mean diameter of NPs was in the range of 20–30 nm. In the image, the particles were well dispersed without any signs of aggregation, which is consistent with the UV–Vis results.

The elemental composition of CuO NPs@Starch nanocomposite was determined by EDX analysis. As depicted in Fig. 5, the profile displays and confirms the presence of Cu in the composite. Again, the signals corresponding to C and O atoms can be ascribed to starch molecule thereby assuring the proposed nanostructure. Also the sample FE-SEM mapping was assessed as well (Fig. 6). Considering the compositional maps

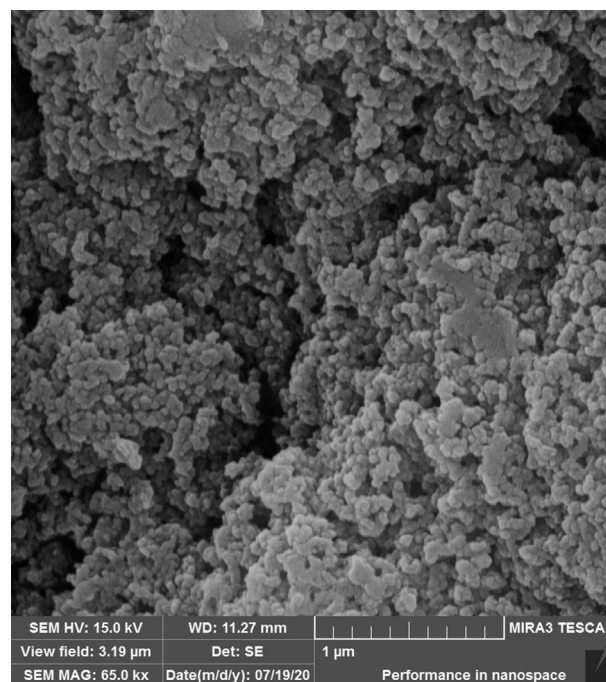


Fig. 3 FE-SEM image of CuO NPs@Starch nanocomposite.

Cu, O and C, the CuO NPs existence with excellent dispersion are analyzed in the composite.

Fig. 7 reveals the pattern of the material XRD, which clearly shows the crystalline nature of the CuO NPs@Starch nanocomposite. The Bragg's peaks of starch are observed at  $15.14^\circ$ ,  $17.31^\circ$ ,  $18.22^\circ$ ,  $20.05^\circ$  and  $23.32^\circ$  ( $2\theta$ ) and matches with literature reports (Castano et al.; Yu et al., 2013). The observed diffraction peaks position at  $32.58^\circ$ ,  $35.62^\circ$ ,  $38.77^\circ$ ,  $48.81^\circ$ ,  $53.53^\circ$ ,  $58.37^\circ$ ,  $61.60^\circ$ ,  $66.30^\circ$ ,  $68.15^\circ$ ,  $72.45^\circ$  and  $75.31^\circ$  were assigned to (110), ( $-111$ ), (111), ( $-202$ ), (020), (202), ( $-113$ ), ( $-311$ ), (220), (311) and ( $-222$ ) are highly consistent with JCPDS standard no. 01-080-0076 of

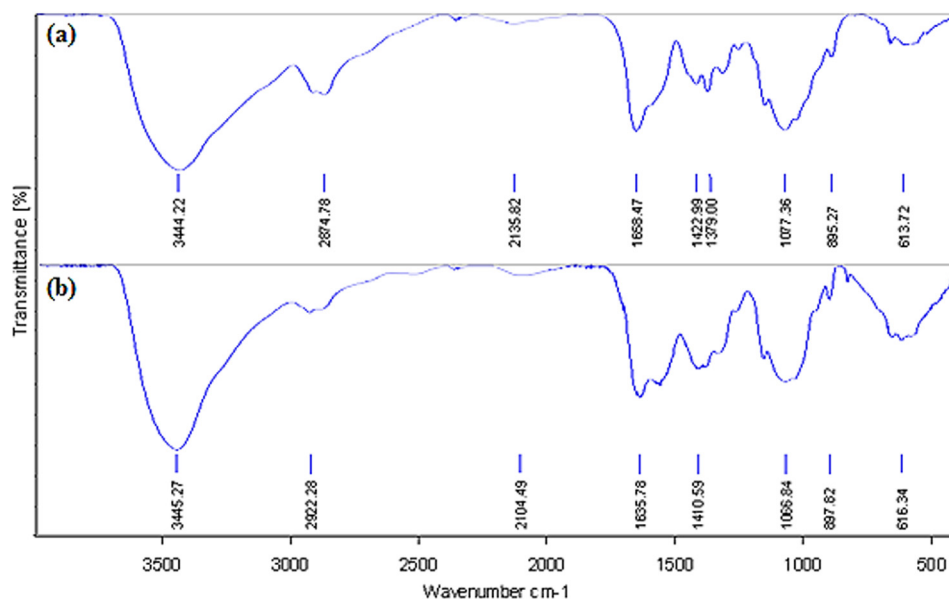


Fig. 2 FT-IR analysis of starch (a) and CuO NPs@Starch nanocomposite (b).

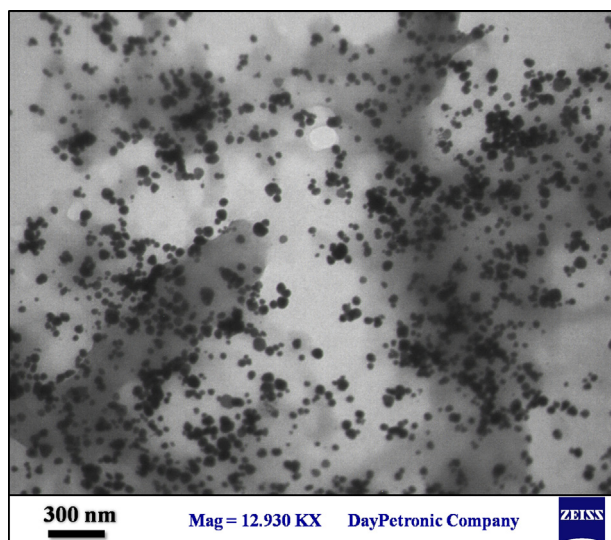


Fig. 4 TEM image of CuO NPs@Starch nanocomposite.

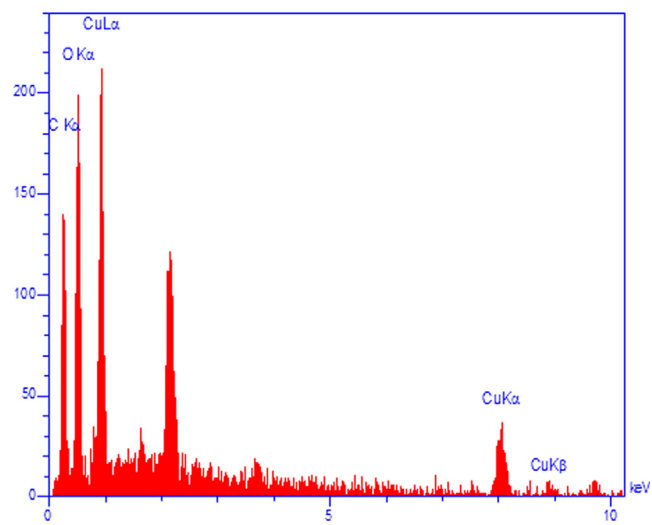


Fig. 5 EDX spectrum of the CuO NPs@Starch nanocomposite.

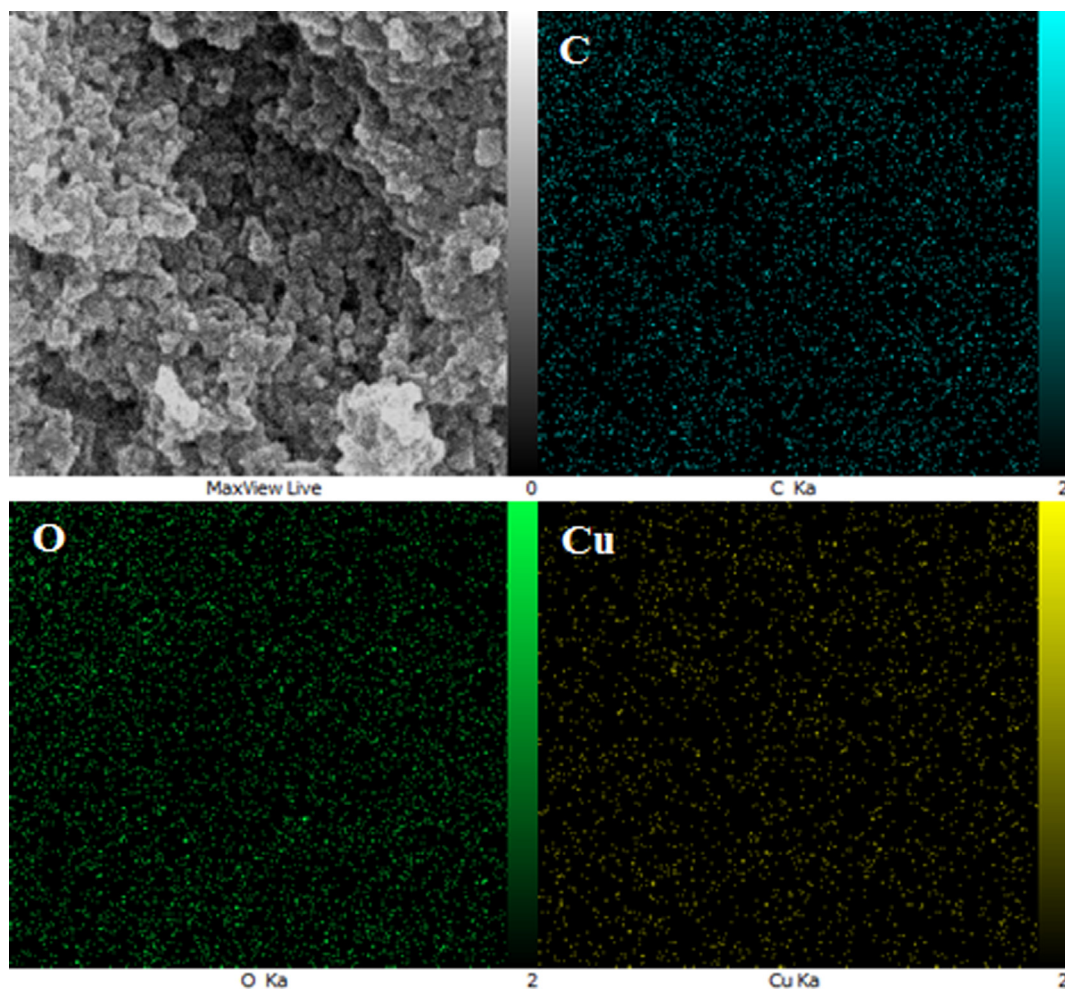


Fig. 6 FE-SEM image of CuO NPs@Starch nanocomposite with its elemental mapping of C, O and Cu respectively.

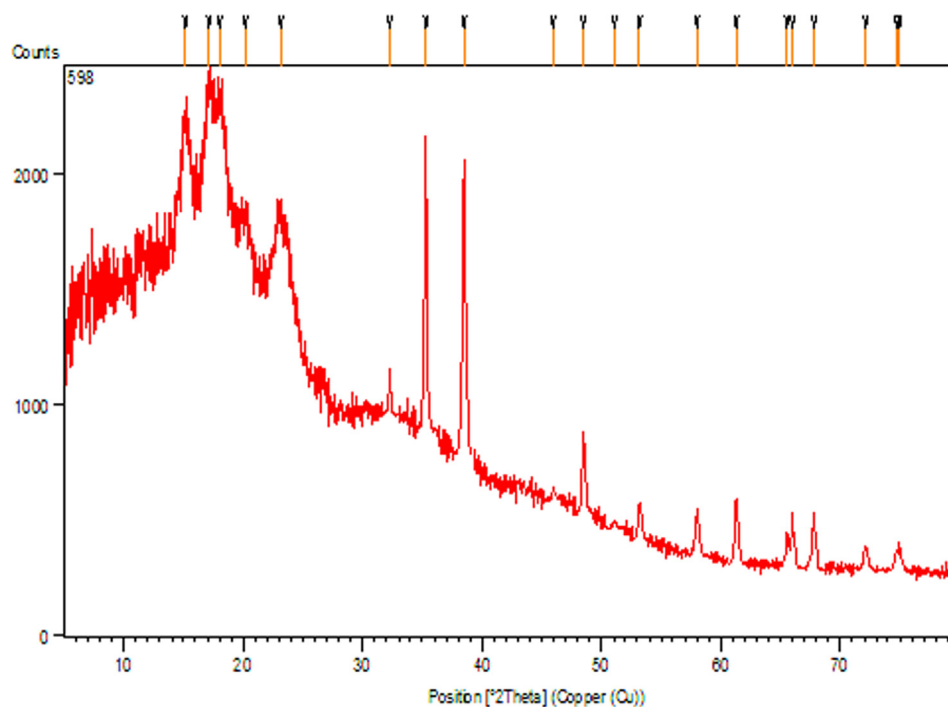


Fig. 7 X-ray diffraction analysis of CuO NPs@Starch nanocomposite.

CuO NPs with a monoclinic phase (Veisi et al., 2021b, Nagajyothi et al., 2017).

### 3.2. Antioxidant properties of CuO NPs@Starch

At least one of the influential factors in many metabolic disorders is oxidative stress factors. Therefore, preventing the production or elimination of stressors can be effective in preventing or improving related diseases. For example, free radicals and oxidative stress play a key role in developing amyloid beta neurotoxicity in the onset of Alzheimer's disease (Nagajyothi et al., 2017; Namvar et al., 2014; Sankar et al., 2014; Beheshtkhoo et al., 2018; Radini et al., 2018; Katata-Seru et al., 2018). The benefits of antioxidants range from preventing heart disease to reducing damage to the brain and eyes (Nagajyothi et al., 2017). Antioxidants block and neutralize the action of free radicals, which are active and destructive substances. The production of free radicals is a natural problem and occurs during the process of respiration (Namvar et al., 2014; Sankar et al., 2014). If many free radicals are suddenly produced in the body, it triggers a series of specific reactions in a row. Free radicals react with certain parts of the cell, such as DNA and cell membranes, causing cell damage or even death (Sankar et al., 2014; Beheshtkhoo et al., 2018; Radini et al., 2018). Normally, the body's immune sys-

tem neutralizes these free radicals. But destructive environmental agents such as environmental, ultraviolet rays, and alcohol pollution make the body unable to fight these free radicals (Nagajyothi et al., 2017; Namvar et al., 2014; Sankar

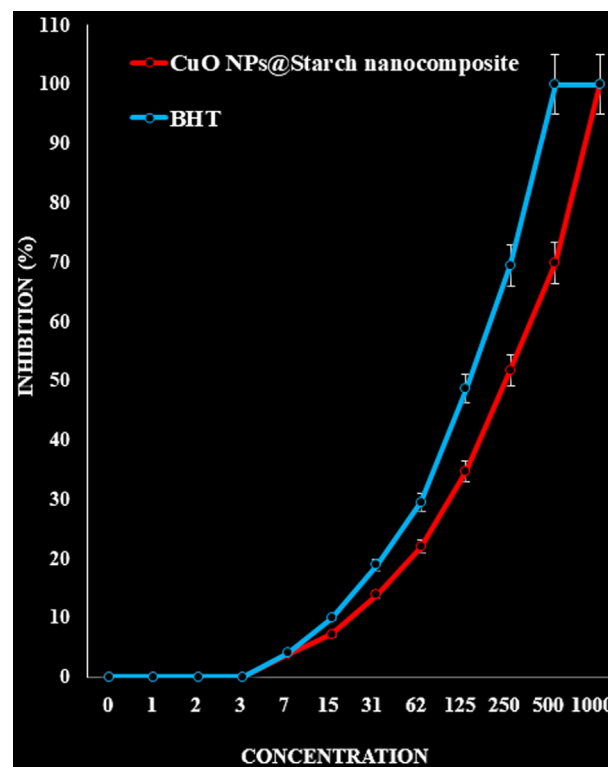


Fig. 8 The antioxidant activities of CuO NPs@Starch nanocomposite and BHT against DPPH.

et al., 2014; Beheshtkhoo et al., 2018; Radini et al., 2018). As a result, the structure and function of body cells are destroyed by free radicals, leading to premature aging and diseases such as cancer and heart disease (Sankar et al., 2014; Beheshtkhoo et al., 2018). Free radicals react with certain parts of the cell, such as DNA and cell membranes, causing cell damage or even death. In this case, these radicals are harmful and dangerous to the health of the body (Namvar et al., 2014; Sankar et al., 2014). To prevent these atoms from working, the body must have a defense barrier against antioxidants. Antioxidants block the free radicals action and prevent the vital cells destruction. Preventing cell damage inhibits diseases such as cardiovascular disease, cancer, and skin aging (Sankar et al., 2014; Beheshtkhoo et al., 2018). Consumption of more antioxidants provides the basis for the body to easily eliminate harmful free radicals. Recent studies have shown that metal nanoparticles have unique antioxidant properties (Namvar et al., 2014; Sankar et al., 2014; Beheshtkhoo et al., 2018; Radini et al., 2018).

In this study, we assessed the antioxidant properties of CuO NPs@Starch nanocomposite by using the DPPH test as a common free radical. DPPH method is one of the most widely used methods for estimating antioxidant content. DPPH is a stable radical that reacts with hydrogen atom compounds. This test is based on the inhibition of DPPH, which causes the decolorization of DPPH solution by adding radical species or antioxidants. DPPH changes color from purple to yellow by taking an electron from the antioxidant compound. The free radicals in DPPH are adsorbed at 517 nm, which follows Beer Lambert's law, and decreased absorption is linearly related to the amount of antioxidants; the higher the amount of antioxidants, the more DPPH is consumed and the more purple turns yellow (Veisi et al., 2021b).

The scavenging capacity of CuO NPs@Starch nanocomposite and BHT at different concentrations expressed as percentage inhibition has been indicated in Fig. 8. In the antioxidant test, the IC<sub>50</sub> of CuO NPs@Starch nanocomposite and BHT against DPPH free radicals were 300 and 265 µg/mL, respectively (Table 1 and Fig. 8).

### 3.3. Anti-cancer effects analysis of CuO NPs@Starch

Common cancer treatments, including chemotherapy, radiation and surgery, may reduce the size of the tumor, but the effect of these methods is transient and has no positive effect on patient survival (Sangami and Manu, 2017; Yang et al., 2011; Xinli, 2012; Allen, 2002; Byrne et al., 2008). Therefore, replacing more effective, more specific therapies with fewer side effects with higher anti-cancer activity is a dominant issue in clinical oncology (Allen, 2002; Byrne et al., 2008; Gao et al., 2015; Mohammed et al., 2016; Li, 2014). The gradual maturation of nanotechnology has been considered not only for treat-

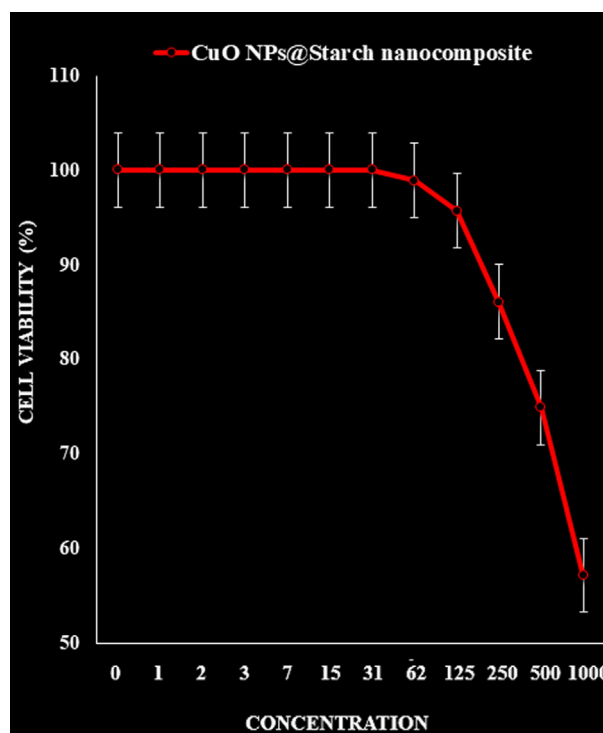


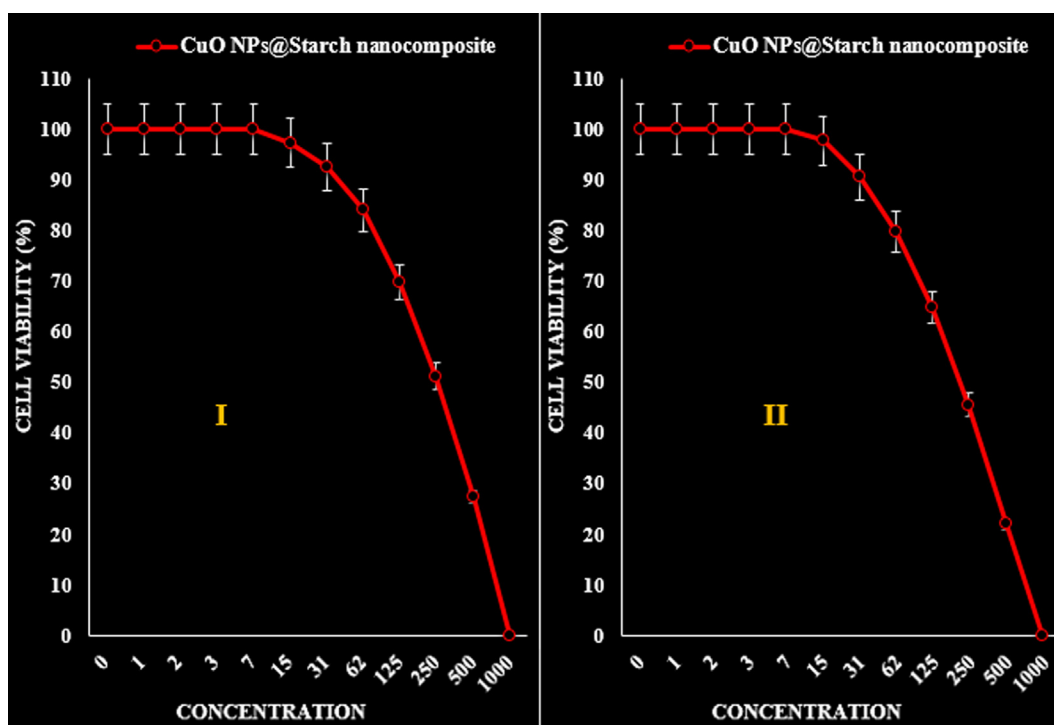
Fig. 9 The cytotoxicity effects of CuO NPs@Starch nanocomposite against normal (HUVEC) cell line.

ing cancer but also for a wide variety of applications, especially for drug delivery and diagnostic and imaging cases. There are many types of nanoparticles available and choosing the right carriers according to demand is a key issue (Li, 2014; Torchilin, 2007; Pranali, 2013; Zhang et al., 2014). Nanoparticles are very close in size to biological molecules in terms of size and can easily penetrate into the cell, for this reason, one of the goals of nanotechnology is to mount molecules and drugs on nanoparticles and transfer them to the target cell (Li, 2014; Torchilin, 2007; Pranali, 2013; Zhang et al., 2014). It is also possible to create different surface properties for nanoparticles by attaching protective ligands to increase the nanoparticles' resistance to the immune system and increase their presence in the bloodstream, and even binding ligands to specifically bind the nanoparticles to the target tissue (Pranali, 2013; Zhang et al., 2014; Gao et al., 2002; Davis et al., 2008; Matsumura et al., 2004).

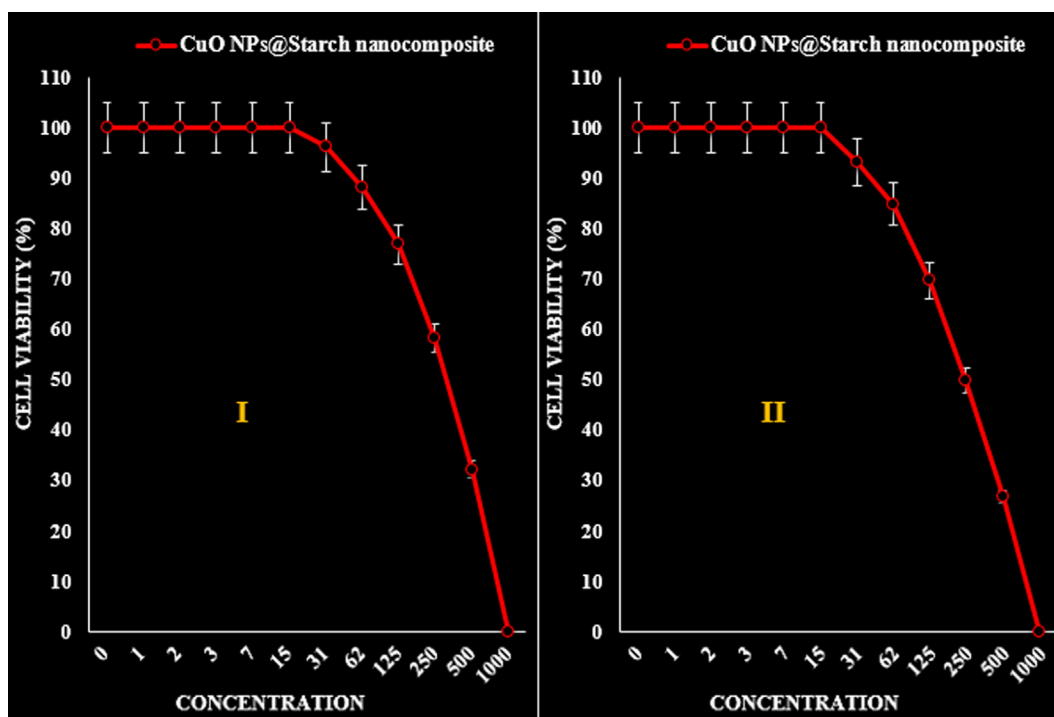
One of the cytotoxicity test methods to measure the rate of cell death is the MTT method, which is based on the formation of formazan dye by reducing the substance MTT (dimethyl thiazole 2 and 5 diphenyltetrazolium bromide) or other tetrazolium salts (Veisi et al., 2021). By breaking the MTT tetrazolium ring by mitochondrial enzymes in living cells, insoluble purple formazan crystals are formed. The formation of these crystals indicates the activity of respiratory chain enzymes and is a measure of cell viability. By measuring the amount of absorption by spectrophotometer at specific wavelengths, the number of living cells can be determined. This test is performed according to ISO 10993-5 and its purpose is in vitro evaluation of cytotoxicity. Cytotoxicity test is performed according to ISO10993-5 standard and in three ways:

Table 1 The IC<sub>50</sub> CuO NPs@Starch nanocomposite and BHT in antioxidant test.

	CuO NPs@Starch nanocomposite (µg/mL)	BHT (µg/mL)
IC <sub>50</sub> against DPPH	236 ± 0 <sup>b</sup>	132 ± 0 <sup>a</sup>



**Fig. 10** The anti-gastric cancer (AGS (I) and KATO III (II)) activities (Cell viability (%)) of CuO NPs@Starch nanocomposite.



**Fig. 11** The anti-pancreatic cancer (AsPC-1 (I) and MIA PaCa-2 (II)) activities (Cell viability (%)) of CuO NPs@Starch nanocomposite.

NRU test, CFU test, MTT test and XTT test. The most common method for assessing cytotoxicity is to measure cell survival by MTT (Veisi et al., 2021b). The basis of MTT method is based on the intensity of dye produced by the mito-

chondrial activity of cells, that measured at a wavelength of 540 to 630 nm and directly proportional to the number of living cells, the increase or decrease in the number of living cells is linearly related to the activity of cell mitochondria. MTT

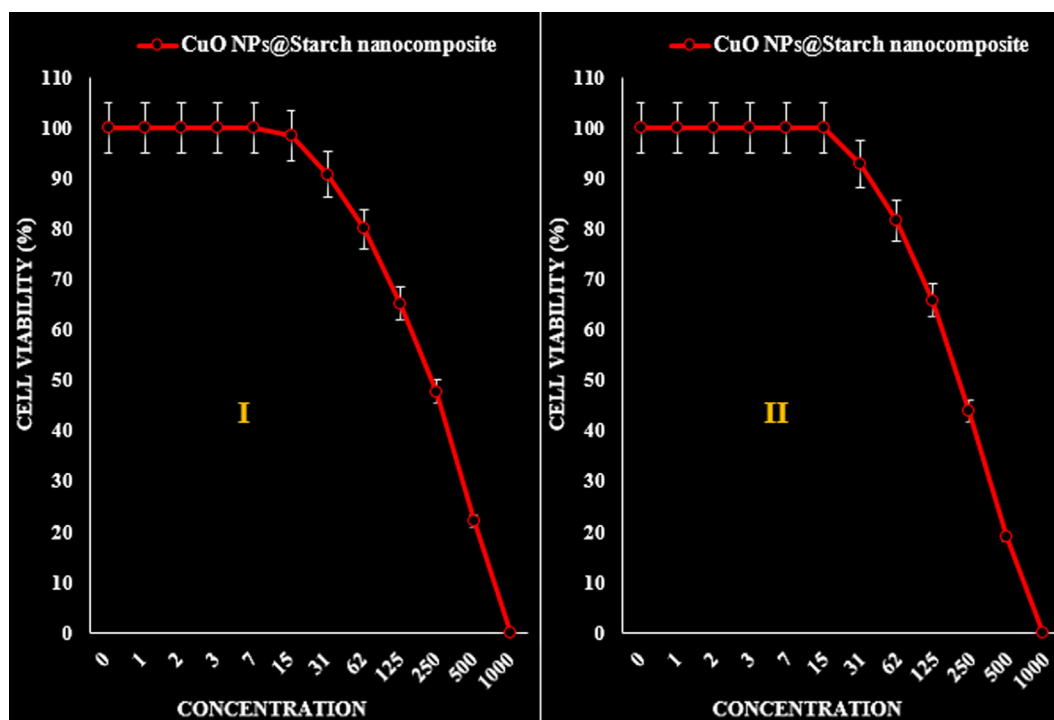


**Fig. 12** The anti-colon cancer (HCT 116 (I) and HCT-8 (II)) activities (Cell viability (%)) of CuO NPs@Starch nanocomposite.

tetrazolium dye is revived in active (metabolically) cells. Mitochondrial dehydrogenases in living cells produce NADH and NADPH, leading to an insoluble purple precipitate called formazan. This precipitate can be dissolved by isopropanol or dimethyl sulfoxide (Veisi et al., 2021b). Dead cells, on the other hand, are unable to perform this conversion due to the inactivity of their mitochondria and therefore do not show a signal. In this method, dye formation is used as a marker for the presence of living cells. In recent years, MTT testing has been the most important measurement method to evaluate the toxicity and anti-cancer effects of metal nanoparticles (Veisi et al., 2021b).

In this investigation, the treated cells with different concentrations of the present CuO NPs@Starch nanocomposite were assessed by MTT assay for 48 h about the cytotoxicity properties on normal (HUVEC) and gastric cancer (AGS and KATO III), pancreatic cancer (AsPC-1 and MIA PaCa-2), and colon cancer (HCT 116 and HCT-8) (Figs. 9–12).

The absorbance rate was evaluated at 570 nm, which represented viability on normal cell line (HUVEC) even up to 1000 µg/mL for CuO NPs@Starch nanocomposite (Tables 2–4 and Fig. 9).

**Table 2** The IC<sub>50</sub> of CuO NPs@Starch nanocomposite in the anti-gastric cancer test.

	CuO NPs@Starch nanocomposite (µg/mL)
IC <sub>50</sub> against HUVEC	–
IC <sub>50</sub> against AGS	262 ± 0 <sup>a</sup>
IC <sub>50</sub> against KATO III	221 ± 0 <sup>a</sup>

The viability of malignant cancer cell lines (gastric cancer (AGS and KATO III), pancreatic cancer (AsPC-1 and MIA PaCa-2), and colon cancer (HCT 116 and HCT-8)) reduced dose-dependently in the presence of CuO NPs@Starch nanocomposite (Tables 2–4 and Figs. 10–12).

It appears that the anti-cancer effect of CuO NPs@Starch nanocomposite is due to their antioxidant effects. Because tumor progression is so closely linked to inflammation and oxidative stress, a compound with anti-inflammatory and antioxidant properties can be an anticarcinogenic agent (Namvar et al., 2014; Sankar et al., 2014; Beheshtkhoo et al., 2018; Radini et al., 2018; Katata-Seru et al., 2018).

#### 4. Conclusion

In summary, we report the green synthesis of CuO NPs@Starch nanocomposite by depositing *in situ* bioreduced CuO NPs over starch in alkaline medium. The material was physicochemically characterized using UV–Vis and FT-IR spectroscopy, FESEM, TEM, XRD and EDX analysis. Average diameters of the particles were ~ 20–30 nm. The Starch/Au

**Table 3** The IC<sub>50</sub> of CuO NPs@Starch nanocomposite in the anti-pancreatic cancer test.

	CuO NPs@Starch nanocomposite (µg/mL)
IC <sub>50</sub> against HUVEC	–
IC <sub>50</sub> against AsPC-1	329 ± 0 <sup>b</sup>
IC <sub>50</sub> against MIA PaCa-2	250 ± 0 <sup>a</sup>

**Table 4** The IC50 of CuO NPs@Starch nanocomposite in the anti-colon cancer test.

	CuO NPs@Starch nanocomposite (µg/mL)
IC50 against HUVEC	–
IC50 against HCT 116	234 ± 0 <sup>a</sup>
IC50 against HCT-8	215 ± 0 <sup>a</sup>

NPs was assessed in biological applications like cytotoxicity and anticancer activities against gastric cancer (AGS and KATO III), pancreatic cancer (AsPC-1 and MIA PaCa-2), and colon cancer (HCT 116 and HCT-8). The viability of malignant cancer cell line reduced dose-dependently in the presence of CuO NPs@Starch nanocomposite. The CuO NPs@Starch nanocomposite showed the best antioxidant activities against DPPH. It seems that the anti-cancer effect of recent nanoparticles is due to their antioxidant effects.

#### Acknowledgment

The authors extend their appreciation to the Deanship of Scientific Research at King Khalid University for funding this work through General Research Project under grant number (RGP. 2/88/42).

#### Funding

The National Nature Science Foundation of China (face items) (NO. 81572363).

#### References

- Borm, P.J., Robbins, D., Haubold, S., et al, 2006. The potential risks of nanomaterials: a review carried out for ECETOC. *Particle Fibre Toxicol.* 3 (1), 11.
- De Jong, W.H., Borm, P.J., 2008. Drug delivery and nanoparticles: applications and hazards. *Int. J. Nanomed.* 3 (2), 133–149.
- Mao, B.H. et al, 2016. Mechanisms of silver nanoparticle-induced toxicity and important role of autophagy. *Nanotoxicol* 10, 1021–1040.
- You, C., Han, C., Wang, X., et al, 2012. The progress of silver nanoparticles in the antibacterial mechanism, clinical application and cytotoxicity. *Mol. Biol. Rep.* 39, 9193–9201. <https://doi.org/10.1007/s11033-012-1792-8>.
- (a) Trojer MA, Li Y, Wallin M, Holmberg K, Nyden M. Charged microcapsules for controlled release of hydrophobic actives Part II: surface modification by LbL adsorption and lipid bilayer formation on properly anchored dispersant layers. *J Colloid Interface Sci.* 2013; 409:8-17; (b) Z. Karimi Ghezeli, M. Hekmati, H. Veisi, Synthesis of Imatinib-loaded chitosan-modified magnetic nanoparticles as an anti-cancer agent for pH responsive targeted drug delivery. *Applied Organometallic Chemistry* 33 (2019) e4833; (c) R. Ghorbani-Vaghei, S. Hemmati, M. Hekmati, Pd immobilized on modified magnetic Fe<sub>3</sub>O<sub>4</sub> nanoparticles: Magnetically recoverable and reusable Pd nanocatalyst for Suzuki-Miyaura coupling reactions and Ullmann-type N-arylation of indoles, *Journal of Chemical Sciences* 128 (2016) 1157-1162; (d) Wei Zhang, Hojat Veisi, Reyhaneh Sharifi, Delafarin Salamat, Bikash Karmakar, Malak Hekmati, Saba Hemmati, Mohammad Mahdi Zangeneh, Zhiyong

- Zhang, Qiang Su, Fabrication of Pd NPs on pectin-modified Fe<sub>3</sub>O<sub>4</sub> NPs: A magnetically retrievable nanocatalyst for efficient C–C and C–N cross coupling reactions and an investigation of its cardiovascular protective effects, *Int J Biological Mac.* 160 (2020) 1252-1262; (e) S. Abbasi, M. Functionalization of multi-walled carbon nanotubes with pramipexole for immobilization of palladium nanoparticles and investigation of catalytic activity in the Sonogashira coupling reaction. *Appl. Organomet. Chem.* 31 (2017) e3600; (f) S. Taheri, H. Veisi, M. Hekmati, Application of polydopamine sulfamic acid-functionalized magnetic Fe<sub>3</sub>O<sub>4</sub> nanoparticles (Fe<sub>3</sub>O<sub>4</sub>@PDA-SO<sub>3</sub>H) as a heterogeneous and recyclable nanocatalyst for the formylation of alcohols and amines under solvent-free conditions. *New J Chem* 41 (2017) 5075-5081; (g) J. Akbari, M. Hekmati, M. Sheykhani, Guanidine derived ionic liquids: catalyst free medium for N-Formylation of amines, *Polyhedron* 11 (2009) 123-129; (h) 20. H. Veisi, B. Karmakar, T. Tamoradi, S. Hemmati, M. Hekmati, M. Hamelian, Biosynthesis of CuO nanoparticles using aqueous extract of herbal tea (*Stachys Lavandulifolia*) flowers and evaluation of its catalytic activity, *Sci. Rep.* 11 (2021) 1983.
- Liu, D., Chen, L., Jiang, S., et al, 2014. Formulation and characterization of hydrophilic drug diclofenac sodium-loaded solid lipid nanoparticles based on phospholipid complexes technology. *J. Liposome Res.* 24 (1), 17–26.
- Tong, A.M., Lu, W.Y., Xu, J.H., Lin, G.Q., 2004. *Bioorg. Med. Chem. Lett.* 14, 2095–2097.
- (a) T. Baran, I. Sargin, M. Kaya, A. Menteş, T. Ceter, J. *Colloid Interface Sci.* 486 (2017) 194–203; (b) H. Veisi, A. Sedrpoushan, A. R. Faraji, M. Heydari, S. Hemmati, B. Fatahi, *RSC Advances* 5 (2015) 68523-68530; (c) H. Veisi, P. Safarimehr, S. Hemmati, *Materials Science and Engineering: C* 96 (2019) 310-318; (d) H. Veisi, B. Maleki, M. Hamelian, S.S. Ashrafi, *RSC Advances* 5 (2015) 6365-6371; (e) H. Veisi, A.A. Manesh, N. Eivazi, A.R. Faraji, *RSC Advances* 5 (2015), 20098-20107; (f) B. Maleki, S. Hemmati, A. Sedrpoushan, S.S. Ashrafi, H. Veisi, *RSC Advances* 4 (2014), 40505-40510; (g) S. Hemmati, L. Mehrazin, M. Pirhayati, H. Veisi, *Polyhedron* 158 (2019) 414-422; (h) M. Baghayeri, A. Amiri, Z. Alizadeh, H. Veisi, E.Hasheminejad, *Journal of Electroanalytical Chemistry* 810 (2018) 69-77; (i) S. Hemmati, L. Mehrazin, M. Pirhayati, H. Veisi, *Polyhedron* 158 (2019) 414-422; (j) H Veisi *Synthesis* 15 (2010) 2631-2635; (k) M. Hamelian, K. Varmira, H. Veisi, *Journal of Photochemistry and Photobiology B: Biology* 184 (2018) 71-79.
- Wang, X., Hu, P., Xue, F., Wei, Y., 2014. *Carbohydr. Polym.* 114, 476–483.
- H. Elkhenany, M. Abd Elkodous, N.I. Ghoneim, T.A. Ahmed, S.M. Ahmed, I.K. Mohamed, N. El-Badri, *Int. J. Biol. Macromol.* 143 (2020) 763–774.
- Veisi, H., Joshani, Z., Karmakar, B., Tamoradi, T., Heravi, M.M., Gholami, J., 2021a. *Int. J. Biol. Macromol.* 172, 104–113.
- Budarin, V.L., Clark, J.H., Luque, R., Macquarrie, D.J., White, R.J., 2008. *Green Chem.* 10, 382–387.
- Shaabani, A., Rahmati, A., Badri, Z., 2008. *Catal. Commun.* 9, 13–16.
- Lu, Y., Wan, X., Li, L., Sun, P., Liu, G., 2021. Synthesis of a reusable composite of graphene and silver nanoparticles for catalytic reduction of 4- nitrophenol and performance as anti-colorectal carcinoma. *J. Mater. Res. Technol.* 12, 1832–1843.
- Veisi, H., Karmakar, B., Tamoradi, T., Hemmati, S., Hekmati, M., Hamelian, M., 2021b. *Sci. Rep.* 11 (1), 1–13.
- J. Castano, S. Rodriguez-Llamazares, K. Contreras, C. Carrasco, C. Pozo. R. Bouza, C. M.
- Yu, H., Cheng, L., Yin, J., Yan, S., Liu, K., Zhang, F., Xu, B., Li, L., 2013. *Food. Sci. Nutr.* 1 (4), 273–283.
- Nagajyothi, P.C., Muthuraman, P., Sreekanth, T.V.M., Kim, D.H., Shim, J., 2017. *Arab. J. Chem.* 10, 215–225.
- Namvar, F., Rahman, H.S., Mohamad, R., et al, 2014. Cytotoxic effect of magnetic iron oxide nanoparticles synthesized via seaweed aqueous extract. *Int J Nanomedicine* 19, 2479–2488.

- Sankar, R., Maheswari, R., Karthik, S., et al. 2014. Anticancer activity of *Ficus religiosa* engineered copper oxide nanoparticles. *Mat Sci Eng C* 44, 234–239.
- Beheshtkhoo, N., Kouhbanani, M.A.J., Savardashtaki, A., et al. 2018. Green synthesis of iron oxide nanoparticles by aqueous leaf extract of *Daphne mezereum* as a novel dye removing material. *Appl. Phys. A* 124, 363–369.
- Radini, I.A., Hasan, N., Malik, M.A., et al. 2018. Biosynthesis of iron nanoparticles using *Trigonella foenum-graecum* seed extract for photocatalytic methyl orange dye degradation and antibacterial applications. *J. Photochem. Photobiol., B* 183, 154–163.
- Katata-Seru, L., Moremedi, T., Aremu, O.S., et al. 2018. Green synthesis of iron nanoparticles using *Moringa oleifera* extracts and their applications: Removal of nitrate from water and antibacterial activity against *Escherichia coli*. *J. Mol. Liq.* 256, 296–304.
- Sangami, S., Manu, M., 2017. Synthesis of Green Iron Nanoparticles using Laterite and their application as a Fenton-like catalyst for the degradation of herbicide Ametryn in water. *Environ. Technol. Innov.* 8, 150–163.
- Yang, F., Jin, C., Jiang, Y., et al. 2011. Liposome based delivery systems in pancreatic cancer treatment: from bench to bedside. *Cancer Treat. Rev.* 37 (8), 633–642.
- Xinli, D.H.Z.S., 2012. Applications of nanocarriers with tumor molecular targeted in chemotherapy. *Chemistry.* 75 (7), 621–627.
- Allen, T.M., 2002. Ligand-targeted therapeutics in anticancer therapy. *Nat. Rev. Cancer* 2 (10), 750–763.
- Byrne, J.D., Betancourt, T., Brannon-Peppas, L., 2008. Active targeting schemes for nanoparticle systems in cancer therapeutics. *Adv. Drug Del. Rev.* 60 (15), 1615–1626.
- Gao, J., Wang, Z., Liu, H., Wang, L., Huang, G., 2015. Liposome encapsulated of temozolomide for the treatment of glioma tumor: preparation, characterization and evaluation. *Drug Discov Ther.* 9 (3), 205–212.
- Mohammed, M.I., Makky, A.M., Teaima, M.H., Abdellatif, M.M., Hamzawy, M.A., Khalil, M.A., 2016. Transdermal delivery of vancomycin hydrochloride using combination of nano-ethosomes and iontophoresis: in vitro and in vivo study. *Drug Deliv.* 23 (5), 1558–1564.
- Li YN, G F. Recent progress in doxorubicin nano-drug delivery systems for reserving multidrug resistance. 2014; 11(3):177-181.
- Torchilin, V.P., 2007. Targeted pharmaceutical nanocarriers for cancer therapy and imaging. *AAPS J.* 9, E128–E147.
- Pranali, P., 2013. Deshpande, Current trends in the use of liposomes for tumor targeting. *Nanomedicine* 8 (9), 1509–1528.
- Zhang, Y., Huang, Y., Li, S., 2014. Polymeric micelles: Nanocarriers for cancer-targeted drug delivery. *AAPS PharmSciTech* 15, 862–871.
- Gao, Z., Lukyanov, A.N., Singhal, A., Torchilin, V.P., 2002. Diacyl-lipid-polymer micelles as nanocarriers for poorly soluble anticancer drugs. *Nano Lett.* 2 (9), 979–982.
- Davis, M.E., Chen, Z., Shin, D.M., 2008. Nanoparticle therapeutics: an emerging treatment modality for cancer. *Nat Rev Drug Discov.* 7 (9), 771–782.
- Matsumura, Y., Hamaguchi, T., Ura, T., Muro, K., Yamada, Y., Shimada, Y., Shirao, K., Okusaka, T., Ueno, H., Ikeda, M., et al. Cancer 2004. Phase I clinical trial and pharmacokinetic evaluation of NK911, a micelle-encapsulated doxorubicin. *Br. J. Cancer* 91, 1775–1781.
- Nie, S., Xing, Y., Kim, G.J., Simons, J.W., 2007. Nanotechnology applications in cancer. *Annu. Rev. Biomed. Eng.* 9, 257–288.